On Modeling Center of Foot Pressure Distortion Through a Medium

Aimee L. Betker, *Member, IEEE*, Zahra M. K. Moussavi*, *Member, IEEE*, and Tony Szturm

***Abstract*—The *center of foot pressure* (COP) is a commonly used output measure of the postural control system as it is indicative of the systems stability. A dense piece of foam, i.e., a sponge, can be used to emulate random environmental conditions that distort the ground reaction forces received and interpreted by the cutaneous sensors in the feet; thus introducing uncertainty into the control system. In this paper, the density and size of the sponge was selected such that a subject's weight did not cause full compression. In general, the COP is measured from the bottom of the sponge. As the sponge is used to distort ground reaction forces, it is reasonable then to assume that the COP signal would also be distorted. The use of other sensory information to identify state of balance, and compute necessary balance adjustments, is therefore required. In addition to a sponge, many different types of specialized footwear and inserts are used for people with peripheral neuropathy, such as diabetics. However, it is difficult to design diabetic footwear without a better understanding of the mechanical and physiological effects that different surfaces typical of outdoor terrains, such as a sponge, which cannot be predicted without the sense of the foot, have on balance. Therefore, the goal of this study was to investigate the change of the COP signal from the top and bottom of the sponge. Portable force sensing mats from Vista Medical were used to obtain the COP from the top and bottom of the sponge. The COP measured on the bottom of the sponge is not the same as the COP measured on the top, particularly in the medial-lateral direction. Several linear and nonlinear models were used to identify the unknown plant; i.e., the sponge. Overall, the nonlinear neural network method had superior performance when compared with the linear models. Thus, the results indicate that the signals from the top and bottom of the sponge are in fact different, and furthermore, they are nonlinearly related. A nonlinear mathematical model is proposed which describes COP distortion through a medium such as a sponge. Although the values for the model parameters determined were for a particular sponge, this study suggests that a neural network plant identification model may be applied to any medium other than the sponge; the information can then be used to determine how the balance control model is affected given the sensory information received.**

***Index Terms*—Adaptive filtering, center of foot pressure, neural network, plant identification, sponge, Wiener filter.**

I. Introduction

BALANCE of the human multi-segmental system requires adequate sensory inputs, which are efficiently organized and integrated by the *central nervous system* (CNS). All three primary sources of spatial information, vestibular, somatosensory and visual inputs, are required in order to distinguish egocentric, visual background, visual target and support surface motions. Each sensory class provides the CNS with specific information about position and motion of the body within its environment. Vision provides relative motion information, vertical and horizontal; external reference frames which are not available in the dark or crowded places. The vestibular system provides an absolute external reference frame, gravitational vertical. Cutaneous sensors provide information about ground and base of support forces, which can be distorted by a variety of natural surfaces. Proprioceptors, such as muscle spindles, provide information about relative position and motion of a body segment to adjacent body segments. The most common surfaces used for balance and walking assessment are fixed, predictable, level and firm support surfaces. However, in order to provide a complete assessment, different surface conditions, such as spongy or cushion surfaces, which can alter the ground reaction forces in an unpredictable manner should also be taken into account [1]. The *center of foot pressure* (COP) is a commonly used output measure of a postural control system [2]–[6]. The *center of mass* (COM) must remain within its base of support, or have the required momentum in the appropriate direction to re-enter the base of support area, or else instability will occur; the COP represents an index of this. Thus the trajectory of the COP provides us with an outcome measure of the balance control system.

A common method of balance assessment uses a force plate with a firm, level support surface. In order to evaluate different balance control mechanisms, these platforms have been sinusoidally translated in the *anterior-posterior* (AP) direction to examine predictive control [2], [7], [8]. These sinusoidal translations are generally periodic, and thus provide predictive control to the simulated environmental change. However, in everyday situations we encounter a variety of different surfaces which do not provide the predictable feedback of the firm surface used in testing. Therefore, the platforms have been servo-controlled relative to center of foot pressure; i.e., sensory organization test [9]. In addition, they can be suddenly translated, in AP and *medial-lateral* (ML) directions, to elicit unexpected balance disturbances [10], [11]. Investigators are now employing a dense piece of foam, or a sponge, as an alternative test surface [1], [5], [6], [12]. The sponge surface emulates uncertainty in the system by randomly altering the ground reaction forces that the

Manuscript received January 14, 2004; revised July 2, 2004. *Asterisk indicates corresponding author.*

A. L. Betker is with the Department of Electrical and Computer Engineering, University of Manitoba, Winnipeg, MB R3T 5V6 Canada (e-mail: abetker@ieee.org).

*Z. M. K. Moussavi is with the Department of Electrical and Computer Engineering, University of Manitoba, 15 Gillson Street, Winnipeg, MB R3T 5V6 Canada (e-mail: mousavi@ee.umanitoba.ca).

T. Szturm is with the School of Medical Rehabilitation, University of Manitoba, Winnipeg, MB R3T 5V6 Canada (e-mail: ptsturm@cc.umanitoba.ca).

Digital Object Identifier 10.1109/TBME.2004.840466

cutaneous sensors of the feet receive. Therefore, the forces will be distorted and delayed versions of the original signal.

Loss of sensation in the feet, as a result of peripheral vascular disease, is a major problem for individuals with diabetes. A variety of footwear, including specially designed cushioning insoles, shoe inserts, rocker bottom designs and orthotic devices, have been prescribed in order to reduce, redistribute and deflect foot pressures during walking [13], [14]. In addition, the footwear is used to support the arch and re-align the forefoot in order to improve the foot mechanics, and in more recent work to enhance the cutaneous signals from the soles of the foot. However, it is difficult to design diabetic footwear without a better understanding of the mechanical and physiological effects that different surfaces typical of outdoor terrains, such as a sponge, which cannot be predicted without the sense of the foot, have on balance.

In this paper, we have simultaneously measured the COP from above and below a dense foam sponge, using a portable force sensing mat, during sinusoidal movement. The sponge can be thought of as representing an unknown plant, which receives as its input the COP signal from the top of the sponge; the output of the plant is the COP as measured from below the sponge. We investigated the use of linear and nonlinear plant identification techniques to develop a mathematical model of the sponge. Specifically, linear inverse modeling, using the adaptive *least mean squares* (LMS) algorithm and the *recursive least squares* (RLS) algorithm to update the weights of an adaptive filter, was used. In addition, a linear Wiener filter was also designed. For the nonlinear model, an adaptive neural network plant model was developed. Overall, the neural network method had superior performance when compared with the linear models. The results are approximately equal to the desired outputs, for both the AP and ML directions. Although the values for the model parameters determined were for a particular sponge, the results suggest that a neural network plant identification model may be applied to any medium other than the sponge.

II. Methodology

A. Subjects

Sixteen healthy subjects (5 females) aged 29 ± 7.6, with no history of postural problems, volunteered to participate and gave informed consent. Ethics approval was granted prior to recruiting subjects by The University of Manitoba, Faculty of Medicine, Ethics Committee.

B. Experimental Setup

A block diagram of the system setup is given in Fig. 1. A 50.8 cm $\times$ 50.8 cm $\times$ 10.16 cm (W $\times$ L $\times$ H) sponge of density 25.31 $\mathrm{kg/m^3}$ and a 25% *indentation force deflection* (IFD) of 31.82 kg was used to emulate environmental uncertainty. This means that a weight of 31.82 kg will cause the sponge to be compressed from 50.8 cm in height to 38.1 cm, or 75% of its original value. The density of the sponge was selected such that a subject's weight did not cause full compression. A 25.4 cm $\times$ 40.64 cm $\times$ 1.91 cm (W $\times$ L $\times$ H) wooden board was placed on top of the sponge to equally distribute the forces applied by the body on the sponge, thus

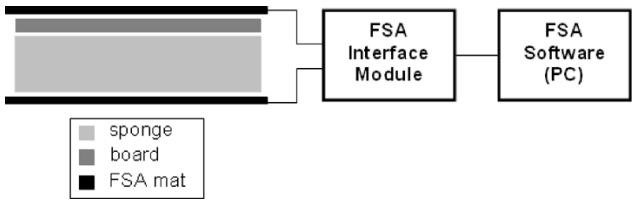

Fig. 1. Block diagram of experimental setup and data acquisition.

minimizing the compression of the sponge and normalizing the effect of differences in body weight. Note that differences in body weight will affect the amount of compression on the sponge, making it difficult to obtain a perfect transfer function. However, in order for the model to be valid for the widest range of human movements and conditions, we incorporated a wide range of movement types and decoupling between COM and COP to test our model. Vertical pressure forces, from below and on top of the sponge, were sampled at 12 Hz utilizing two UltraThin *Force Sensitive Applications* (FSA) OrthoTest Mats (Vista Medical Ltd, 3-55 Henlow Bay, Winnipeg, MB, Canada) connected to an FSA interface module. Each OrthoTest mat was of dimension 53 cm $\times$ 53 cm $\times$ 0.036 cm (W $\times$ L $\times$ H) and contained a 16 by 16 grid of piezo resistive sensors spaced 2.8575 cm apart. The vertical pressure forces for each sensor are equivalent to body mass multiplied by acceleration and have movement in the perpendicular or horizontal plane. As the body mass is constant, the forces at the sensors are proportional to vertical accelerations due to gravity and body motions. Thus, the reference frame is vertical or in the vector direction of acceleration. The COP in the AP and ML planes was then calculated using the FSA software, as the spatial center of all the forces for the given mat [15]. The COP signals were filtered using a fourth-order Butterworth low-pass filter, with a cutoff frequency of 6 Hz [12]. A Seiko Quartz metronome, model SQ44, was used to set the frequency of the subjects voluntary sway at frequencies of 0.33 Hz and 0.67 Hz.

C. Protocol

The subjects stood on a dense sponge with a board placed on top to evenly distribute their mass, with their feet apart at their preferred normal position, and kept their arms crossed in front of their chest. The sponge support surface served to pseudorandomly modify the ground reaction forces under the feet, as the sponge surface cannot accept the normal forces from the feet as the COM moves. Four trials were performed, where the subject was asked to produce two body movements in a sinusoidal fashion at a frequency beat of a metronome, first with eyes open and then eyes closed. Although there exists variability in the way in which balance is maintained, the hip and ankle strategies are the main balance strategies that emerge when a fixed base of support is used [2]. Thus, the first movement emulates a single inverted pendulum model of body sway, known as the ankle movement strategy [10]. The subjects induced AP sway about the ankle joint, with little or no knee and hip rotation at a frequency of approximately 1/3 Hz, with eyes open and eyes closed respectively. The second movement emulates a double inverted pendulum model of body sway, known as the hip strategy [11]. Specifically, the body movements involved flex and extension

of the upper body, head, arms and trunk, with the knee held in extension. The hip strategy was performed in the AP direction at a frequency of approximately 2/3 Hz. Each participant performed 3 to 4 cycles at the indicated frequency before the trial began for practice. The duration of the trials was 25 seconds, with a two minute rest period between each trial.

D. Data Conditioning

The total number of data sets collected was 64; four per subject representing each of the four trials. Each of the input and target vectors were normalized individually, by subtracting their mean and then dividing by their maximum value; this was done to account for position difference between the signals from the top and bottom mats.

III. System Identification

The sponge represents an unknown plant, which receives as its input the COP signal as measured from on top of the sponge, denoted $\mathbf{COP}_{\mathrm{t}}$. The output of the plant is the COP as measured from below the sponge, denoted $\mathbf{COP}_{\mathrm{b}}$. The following sections describe several linear and nonlinear techniques investigated for determining the mathematical characteristics of the sponge.

A. Inverse Modeling: Linear

Inverse modeling involves the use of an adaptive filter to provide a linear model to compensate for the change in the original signal by an unknown plant; in this case, the model was found in the least squares sense. The system setup is given in Fig. 2 [16].

The sponge, with unknown transfer function $\mathbf{H}(z)$, filters $\mathbf{COP}_{\mathrm{t}}$ to produce the center of foot pressure as measured from the bottom of the sponge, $\mathbf{COP}_{\mathrm{b}}$. The adaptive filter then attempts to equalize the difference between $\mathbf{COP}_{\mathrm{b}}$ and the desired output $\mathbf{COP}_{\mathrm{t}}$, by convolving the input with a vector of tap weights $\hat{\mathbf{w}}(n) = [\hat{w}_0(n), \hat{w}_1(n), \ldots, \hat{w}_{M-1}(n)]^{\mathrm{T}}$. The weights are then adjusted according to the least squares difference between the adaptive filter output, the estimated center of foot pressure as measured from on top of the sponge $\mathbf{C\hat{O}P}_{\mathrm{t}}$, and a delayed version of the plant input. When computing the error, the desired output that is compared with the estimated output can be delayed by a factor d (Fig. 2). The plant model then is represented by the inverse of the adaptive filter model. After convergence, $\mathbf{H}(z)$ is given by

$$\mathbf{H}(z) = \frac{1}{\tilde{\mathbf{H}}}(z) \tag{1}$$

where $\tilde{\mathbf{H}}(z)$ is the transfer function of the adaptive filter.

The specific method of weight vector adjustment is dependent upon the algorithm used. In this paper, the adaptive filter was implemented using the LMS and RLS algorithms (Appendix 1). In each case, the leave-one-out method was employed when adapting the filter coefficients, where all except one subject's data (randomly selected) was used in the adaptation of the coefficients. The left out subject's data was then used to test the filter. The adaptation and testing was repeated until each subject's data had been left out. The reported performance is then representative of the average of the test results obtained.

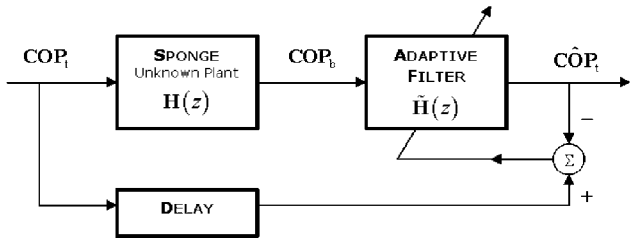

Fig. 2. Block diagram for inverse modeling using adaptive filtering technique.

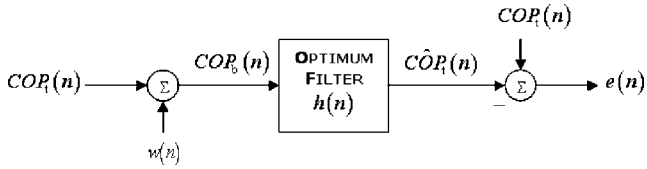

Fig. 3. Block diagram for optimum filter system using Wiener-Hopf technique.

For each of the adaptive filter algorithms, filter orders M of 1, 2, 3, 5, and 7 were used, with delay D in the range [0, M]. It should be noted that for some combinations of filter order and delay, the inverse filter was not stable. The output of the inverse filter was calculated for each of the 64 trials, for each (M, D) combination; the *mean squared error* (MSE) was then calculated for each trial and averaged. Thus, the filter order and delay combination (M, D), along with the corresponding adapted weight vector, with the lowest MSE was selected to represent the inverse transfer function of the sponge.

B. Wiener Filter: Linear

Wiener filter is a linear FIR optimal filter designed to remove noise caused by channel corruption. In the case of this study, the original signal $\mathbf{COP}_{\mathrm{t}}$ becomes corrupted by the channel, i.e., the sponge, and by noise of the measuring process itself, $w(n)$; this produces the signal $\mathbf{COP}_{\mathrm{b}}$ which is then the input to the Wiener filter [16]. The output of the filter is given by

$$\hat{COP}_{\mathrm{t}}(n) = \sum_{\mathrm{k}=0}^{\mathrm{M}-1} h(k)\, COP_{\mathrm{b}}(n-k) \tag{2}$$

where M is the order of the filter, selected as $M = 2$ for this study. A diagram describing a Wiener filter can be seen in Fig. 3. The filter is considered optimal in the *minimum mean squared error* (MMSE) sense, as it minimizes

$$\varepsilon_M = \mathrm{E}\left[|e(n)|^2\right] = \mathrm{E}\left[\left|COP_{\mathrm{t}}(n) - \hat{COP}_{\mathrm{t}}(n)\right|^2\right] \tag{3}$$

where $e(n)$ is the error of the filter [16].

As with the adaptive filters, the leave-one-out method was employed when determining the optimum filter coefficients. The adaptation and testing was repeated until each subject's data had been left out. The reported performance is then representative of the average of the test results obtained. Thus, the determined optimal filter coefficients with the lowest MSE represents the transfer function of the sponge.

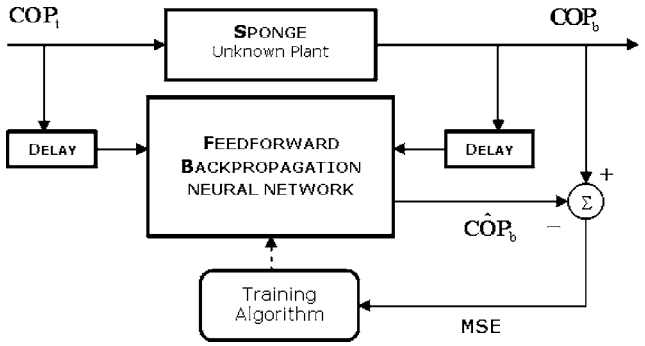

Fig. 4. Block diagram for neural network plant identification.

C. Neural Network Plant Model: Nonlinear

A feedforward backpropagation neural network can be used for nonlinear plant identification in order to derive a formula that represents the characteristics of the sponge [17]. Fig. 4 shows a block diagram of this process. The network uses delayed versions of the plant input and output to estimate the plant output of the current time step. The mean squared error between the estimated and actual plant output is used as the training algorithm's objective function.

A feedforward backpropagation neural network consists of two layers. The first layer, or hidden layer, has a *tangent-sigmoid* (tan-sig) activation function, and the second layer, or output layer, has a linear activation function, purelin. Thus, the first layer limits the output to a narrow range, from which the linear layer can produce all values. The output of each layer can be represented by

$$\mathbf{Y}_{Nx1} = \mathrm{f}(\mathbf{W}_{NxM}\mathbf{X}_{M,1} + \mathbf{b}_{N,1}) \tag{4}$$

where $\mathbf{Y}$ is a vector containing the output from each of the N neurons in a given layer, $\mathbf{W}$ is a matrix containing the weights for each of the M inputs for all N neurons, $\mathbf{X}$ is a vector containing the inputs, $\mathbf{b}$ is a vector containing the biases and $\mathrm{f}(\cdot)$ is the activation function [17]. The network was created using the neural network toolbox from Matlab 6.0 release 12 (The MathWorks, Natick, MA).

In a backpropagation network, there are two steps during training that are performed iteratively, attempting to minimize the mean squared error between the true and estimated plant output. The backpropagation step calculates the error in the gradient descent and propagates it backward to each neuron in the output layer, followed by the hidden layer. In the second step, the weights and biases are recomputed, and the output from the activated neurons is propagated forward from the hidden layer to the output layer.

The network is initialized with random weights and biases, and is then trained using the Levinson–Marquardt algorithm [17]. The weights and biases are updated according to

$$\mathbf{D}_{n+1} = \mathbf{D}_n - \left[\mathbf{J}^{\mathrm{T}}\mathbf{J} + \mu\mathbf{I}\right]^{-1}\mathbf{J}^{\mathrm{T}}e \tag{5}$$

where $\mathbf{D}_n$ is a matrix containing the current weights and biases, $\mathbf{D}_{n+1}$ is a matrix containing the new weights and biases, e is the network error, $\mathbf{J}$ is a Jacobian matrix containing the first derivative of e with respect to the current weights and biases, $\mathbf{I}$ is the identity matrix and μ is a variable that increases or decreases

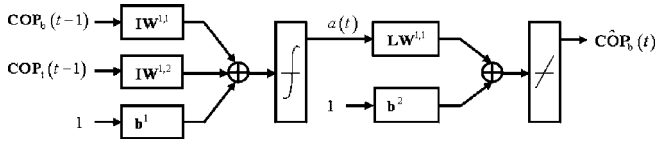

Fig. 5. Block diagram of neural network architecture [16].

based on the performance function. The gradient of the error surface, g, is equal to $\mathbf{J}^{\mathrm{T}}e$ [17].

The architecture of the feedforward backpropagation neural network used to model the plant (sponge) consists of a single neuron in each of the hidden and output layers. The inputs to the network are the center of foot pressure from below the sponge, $\mathbf{COP}_{\mathrm{b}}$, and from on top of the sponge, $\mathbf{COP}_{\mathrm{t}}$, at time $t-1$. The output of the network is the estimated plant output, $\mathbf{COP}_{\mathrm{b}}$, at time t. The neural network architecture is illustrated in Fig. 5.

From the diagram, the overall system equation can be derived. The output of the hidden layer, $a(t)$, is given by

$$a(t) = \mathrm{T}\left[\mathbf{IW}^{1,1}COP_{\mathrm{b}}(t-1) + \mathbf{IW}^{1,2}COP_{\mathrm{t}}(t-1) + \mathbf{b}^1\right] \tag{6}$$

where $\mathrm{T}(\cdot)$ is the tan-sig function, $\mathbf{IW}$ represents the input weights and $\mathbf{b}$ is the bias. The output of the second layer, $\mathbf{C\hat{O}P}_{\mathrm{b}}$, is given by

$$C\hat{O}P_{\mathrm{b}}(t) = \mathrm{P}\left[\mathbf{LW}^{1,1}a(t) + \mathbf{b}^2\right] \tag{7}$$

where $\mathrm{P}(\cdot)$ is the purelin function and $\mathbf{LW}$ represents the layer weight. The overall system equation is then obtained by substituting (6) into (7)

$$C\hat{O}P_{\mathrm{b}}(t) = \mathrm{P}\Bigg(\mathbf{LW}^{1,1}\mathrm{T}\Big[\mathbf{IW}^{1,1}COP_{\mathrm{b}}(t-1) + \mathbf{IW}^{1,2}COP_{\mathrm{t}}(t-1) + \mathbf{b}^1\Big] + \mathbf{b}^2\Bigg). \tag{8}$$

A network for the COP in each of the AP and ML directions must now be trained in order to obtain values for $\mathbf{IW}$, $\mathbf{LW}$ and $\mathbf{b}$.

The training data consisted of 75% of the 64 data sets; 12 sets were randomly selected from each of the four trials. It should be noted that different training sets were used and the network performance was similar for any subset of training data. The test data consisted of the remaining 25% of the data sets. Recall that the data is normalized and thus the vectors lie within the range $[-1,1]$; i.e., the range for which the tan-sig function is most sensitive [17]. Thus, the determined weights and biases for the system described in (8) that result in the lowest MSE represents the nonlinear model of the sponge.

IV. Results

A. Linear Models

The average MSE for each of the linear methods, as well as the model parameters which provided the best results, are given in Table I. As the results for the linear models were similar, the results are plotted for the Wiener filter model only (Figs. 6 and 7).

1) Inverse Modeling: For the LMS algorithm, the output of the plant filter, $\mathbf{C\hat{O}P}_{\mathrm{b}}$, is approximately equal to the input to the filter, $\mathbf{COP}_{\mathrm{t}}$, rather than the desired output, $\mathbf{COP}_{\mathrm{b}}$. Similarly,

TABLE I
MODEL RESULTS

Algorithm	Direction	Model Parameters				MSE (±SD)
		M	D	λ	σ	
LMS	AP	1	0	-	-	0.02 ± 0.01
	ML	1	0	-	-	0.20 ± 0.15
RLS	AP	2	0	0.99	0.0001	0.01 ± 0.01
	ML	1	1	0.9	0.0001	0.11 ± 0.08
Wiener Filter	AP	2	-	-	-	0.01 ± 0.01
	ML	2	-	-	-	0.32 ± 0.22
Nonlinear Network Model	AP	-	-	-	-	0.01 ± 0.005
	ML	-	-	-	-	0.008 ± 0.004

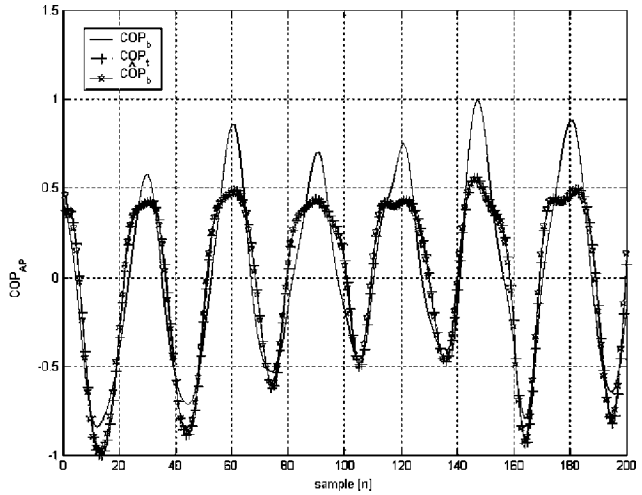

Fig. 6. Plant filter results for the AP direction using a Wiener filter.

for the RLS algorithm, the output of the plant filter, $\hat{\mathbf{COP}}_{\mathrm{b}}$, does not match the desired output $\mathbf{COP}_{\mathrm{b}}$; however, it more closely resembles the desired output than it did for the LMS algorithm. Therefore, the weights of the tap filter could not sufficiently be adapted using the LMS or RLS algorithms; as such, the inverse modeling technique does not show promising results.

2) Wiener Filter: Figs. 6 and 7 show the output of the plant filter for subject 10, trial 1, for the AP and ML directions respectively. The results for this subject are representative of the results obtained for the remaining subjects. For the AP direction, the output of the plant filter, $\hat{\mathbf{COP}}_{\mathrm{b}}$, is approximately equal to the input to the filter, $\mathbf{COP}_{\mathrm{t}}$, rather than the desired output, $\mathbf{COP}_{\mathrm{b}}$. The output of plant filter, $\hat{\mathbf{COP}}_{\mathrm{b}}$, in the ML direction does not follow the input or desired output signal as closely. Therefore, the results were not very promising.

B. Nonlinear Model

The output of the neural plant model was simulated for each of the 64 trials; the MSE was then calculated for the plant model for each trial and averaged.

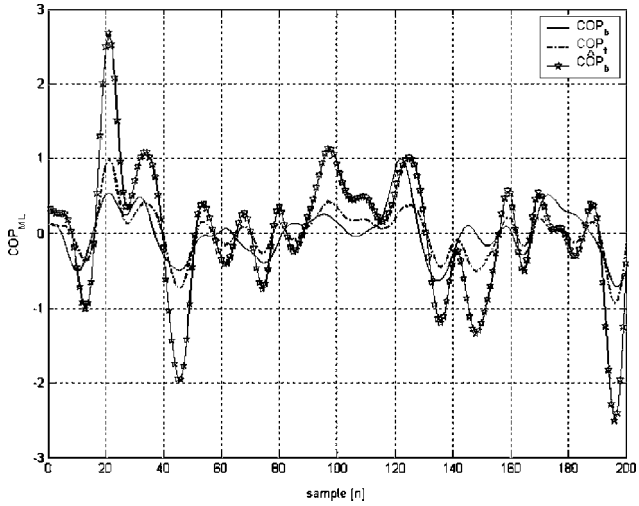

Fig. 7. Plant filter results for the ML direction using a Wiener filter.

TABLE II
NEURAL NETWORK PLANT MODEL PARAMETERS

Direction	Model Parameters				
	$\mathbf{IW}^{1,1}$	$\mathbf{IW}^{1,2}$	$\mathbf{LW}^{1,1}$	$\mathbf{b}^{1}$	$\mathbf{b}^{2}$
AP	0.5775	-0.1134	2.1731	0.0577	-0.1209
ML	-0.2675	$-1.4034e^{-4}$	-3.6718	-0.0178	-0.0649

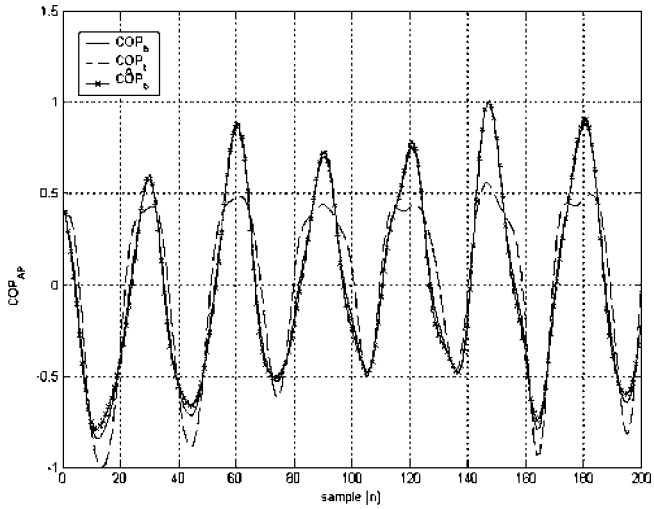

Fig. 8. Neural network plant model results for the AP direction.

For the center of pressure in the AP and ML directions, the MSE was equal to 0.01 ± 0.005 and 0.008 ± 0.004, respectively. The network was trained according to (5) for 28 epochs, when the maximum step size was reached. The values of the input layer and hidden layer bias and weight vectors (obtained after training) are given in Table II. Figs. 8 and 9 show the output of neural network plant model for subject 10, trial 1. The results for this subject are representative of the results obtained for the remaining subjects.

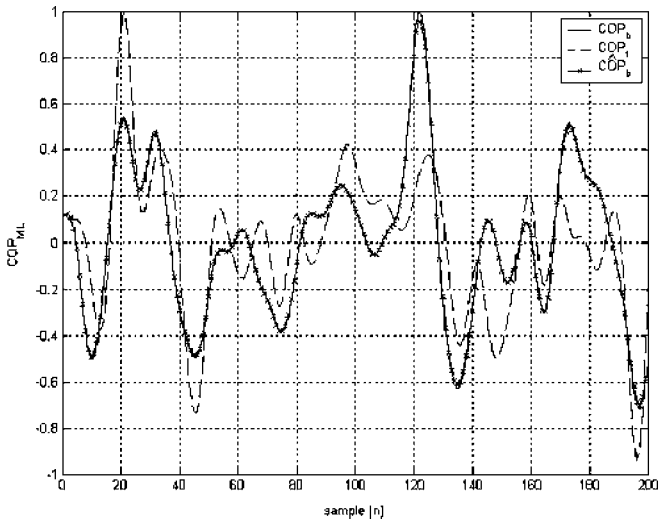

Fig. 9. Neural network plant model results for the ML direction.

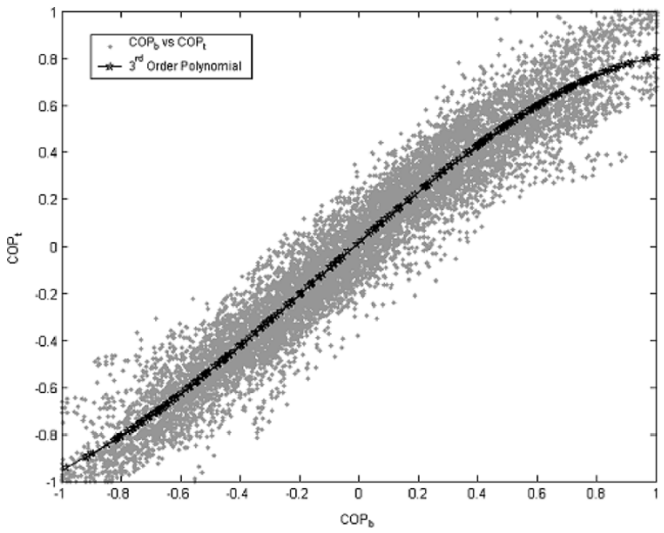

Fig. 10. COP from the bottom of the sponge versus COP from the top of the sponge in the AP direction; a third-order polynomial is fit to the relationship.

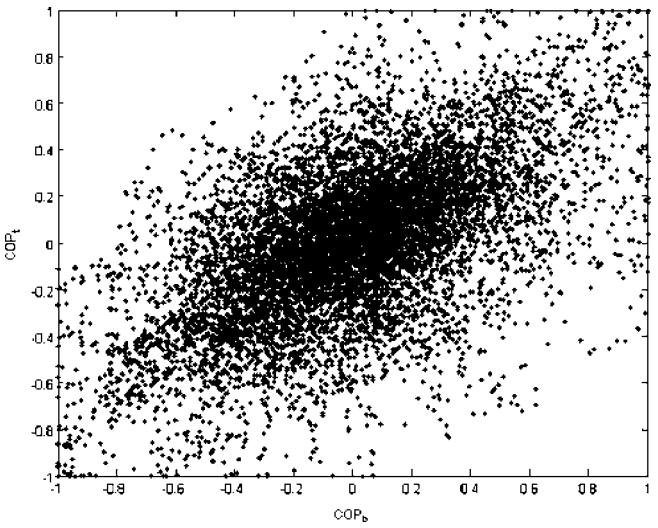

Fig. 11. COP from the bottom of the sponge versus COP from the top of the sponge in the ML direction.

Overall, the neural network method had superior performance when compared with the linear models. The results are approximately equal to the desired outputs, for both the AP and ML directions.

V. Discussion and Conclusion

In general, the COP is usually measured from the bottom of a piece of foam as an outcome balance measure. However, Figs. 6–9 show that the COP measured on the bottom is not the same as the COP measured on the top, particularly in the ML direction. If the $\mathbf{COP}_{\mathrm{b}}$ and $\mathbf{COP}_{\mathrm{t}}$ are linearly related, the COP as measured from below the sponge would only need to be scaled. However, if they are nonlinearly related, then the COP trajectory from the below the sponge is questionable and, hence, this study.

The effects of linear distortion include amplitude scaling and/or phase shifts. Linear models adapt or estimate weights in attempt to equalize the effects of these linear distortions. With the LMS and RLS algorithms, additional user-defined parameters, σ, λ, β, and μ, provide fine tuning of the weights. These parameters can be modified in order to bias the weights toward more favorable outcomes. In this study, however, adjustments of the parameters had little effect on the output of the filter and were not able to characterize all aspects of the signal distortion. Figs. 10 and 11 show the relationship between the $\mathbf{COP}_{\mathrm{b}}$ and $\mathbf{COP}_{\mathrm{t}}$ for the AP and ML directions respectively; for the AP direction, a third-order polynomial curve was fit to the data. These scatter plots indicate that the $\mathbf{COP}_{\mathrm{b}}$ and $\mathbf{COP}_{\mathrm{t}}$ are not related linearly, particularly in the ML direction. This is also reflected in the fact that the linear models developed in this study could not derive a set of filter weights to sufficiently describe the system, suggesting that the relationship between the COP from below and above the sponge is nonlinear.

Conversely, the nonlinear neural network plant model had very low MSE, effectively described the system and was superior to all the applied linear models. Part of the error is partially due to the fact that individuals of different weight would be on a slightly different plant, as the compression and quality of the sponge changes. Substituting the obtained weights and biases (Table II) for the network into (8), the mathematical model for the sponge in the AP and ML directions can be characterized. Note that these values are for the particular foam sponge used in this study, however the model may be used to identify any other surface. Thus the COP as measured from the bottom of the sponge is nonlinearly related to the balance system.

This study suggests that a neural network plant identification model may be applied to any medium other than the sponge and that the information can then be used to determine how the balance control model is affected given the sensory information received.

The analysis of how these different mediums affect foot functions and balance control may also be applied to the development of footwear for diabetics with peripheral neuropathy, prosthetics of amputees and in the elderly. Different insoles, inserts, shoes and orthotic devices have been developed to enhance outdoor walking function, foot mechanics and re-distribution of

TABLE III
LINEAR MODEL FORMULAS

Algorithm	Formula
LMS	$\hat{\mathbf{w}}(n+1) = \hat{\mathbf{w}}(n) + \mu \mathbf{u}(n) e^{*}(n)$ where $\hat{\mathbf{w}}$: weight vector μ : adaptation step size $\mathbf{u}$: input vector $e(n) = COP_t(n-d) - \hat{COP}_t(n)$ d : delay
RLS	$\hat{\mathbf{w}}(n) = \hat{\mathbf{w}}(n-1) + \mathbf{K}(n)\varepsilon^{*}(n)$ $\mathbf{K}(n) = \dfrac{\lambda^{-1}\mathbf{P}(n-1)\mathbf{u}(n)}{1+\lambda \mathbf{u}^{H}(n)\mathbf{P}(n-1)\mathbf{u}(n)}$ $\mathbf{P}(n) = \lambda^{-1}\mathbf{P}(n-1) - \lambda^{-1}\mathbf{K}(n)\mathbf{u}^{H}(n)\mathbf{P}(n-1)$ where ε : $\varepsilon(n) = COP_t(n-d) - \hat{\mathbf{w}}^{H}(n-1)\mathbf{u}(n)$ λ : memory
Wiener filter	$\mathbf{h}_{opt} = \Gamma_{bb}^{-1}\gamma_{tb}$ Where $\mathbf{h}_{opt}$: optimal filter coefficients γ_{bb} : autocorrelation of $\mathbf{COP}_b$ Γ_{bb} : Toeplitz matrix of γ_{bb} γ_{tb} : crosscorrelation between $\mathbf{COP}_t$ and $\mathbf{COP}_b$

contact forces. However it is difficult to design footwear for all of the different surfaces encountered in daily life without considering the effect the surfaces have on the postural control system. The effects of different characteristics for the sponge (e.g., IFD and size), board (e.g., size) and subject (e.g., weight) are also of interest for further investigation. By modeling the force signals as they transfer through different cushioning insoles, positioning inserts and amount of rocker angle, we can determine the degree of somatosensory information the person would receive. It will also allow us to determine the degree of distortion and delay in interpreting the correct adjustments to be made to control COM motion relative to an unstable support base.

In summary, the results of this paper indicate that not only are the COP signals measured from the top and bottom of the sponge different, they are nonlinearly related. A nonlinear mathematical model is defined that describes this relationship.

APPENDIX

In inverse modeling, a vector of tap weights representing the inverse filter's transfer function needs to be adapted; there are two methods used in this study, namely the LMS and RLS algorithms. The LMS and RLS algorithms optimize the filter by adapting the weight vector such that the mean square value of the estimation error is minimized [16]. The RLS differs in that it solves for the minimum least square recursively for each iteration i, where $0 \leq i \leq n$, allowing for quicker convergence than the LMS algorithm [16]. Similarly, the optimal filter coefficients of the Wiener filter need to be determined. Table III gives the formulas for determining the weight vectors for these methods; for a full derivation of the algorithms, refer to [16].

REFERENCES

[1] J. Gill, J. H. J. Allum, M. G. Carpenter, M. H. Ziolkowska, A. L. Adkin, F. Honegger, and K. Pierchala, "Trunk sway measures of postural stability during clinical balance tests: Effects of age," *J. Gerontol.: Med. Sci.*, vol. 56A, no. 7, pp. M438–M447, 2001.

[2] J. J. Buchanan and F. B. Horak, "Emergence of postural patterns as a function of vision and translation frequency," *J. Neurophysiol.*, vol. 6, pp. 2325–2339, 1999.

[3] J. J. Collins and C. J. De Luca, "Open-loop and closed loop control of posture: A random-walk analysis of center-of-pressure trajectories," *Exp. Brain Res.*, vol. 95, pp. 308–318, 1993.

[4] P. Gatev, S. Thomas, T. Kepple, and M. Hallet, "Feedforward ankle strategy of balance during quiet stance in adult," *J. Physiol.*, no. 514.3, pp. 915–928, 1999.

[5] Modified Clinical Test of Sensory Interaction on Balance (mCTSIB). Neurocom International Inc., Clackamas, OR. [Online]. Available: http://www.onbalance.com/neurocom/protocols/sensoryImpairment/mCTSIB.aspx

[6] N. Teasdale, G. E. Stelmach, and A. Breunig, "Postural sway characteristics of the elderly under normal and altered visual and support surface conditions," *J. Gerontol.*, vol. 46, no. 6, pp. B238–244, 1991.

[7] M. Schieppati, A. Giordano, and A. Nardone, "Variability in a dynamic postural task attests ample flexibility in balance control mechanisms," *Exp. Brain Res.*, vol. 144, no. 2, pp. 200–210, 2002.

[8] Y. Ko, J. H. Challis, and K. M. Newell, "Postural coordination patterns as a function of dynamics of the support surface," *Human Movement Sci.*, vol. 20, no. 6, pp. 737–764, 2001.

[9] A. D. Kuo, R. A. Speers, R. J. Peterka, and F. B. Horak, "Effect of altered sensory conditions on multivariate descriptors of human postural sway," *Exp. Brain Res.*, vol. 122, pp. 185–195, 1998.

[10] F. B. Horak and L. M. Nashner, "Central programming of postural movements: Adaptation to altered support-surface configurations," *J. Neurophysiol.*, vol. 55, pp. 1369–1381, 1986.

[11] T. Szturm and B. Fallang, "Effects of varying acceleration of platform translation and toes-up rotations on the pattern and magnitude of balance reactions in humans," *J. Vestibular Res.*, vol. 8, no. 5, pp. 381–397, 1998.

[12] J. H. J. Allum, F. Zamani, A. L. Adkin, and A. Ernst, "Differences between trunk sway characteristics on a foam support surface and on the equitest ankle – Sway–Referenced support surface," *Gait Posture*, vol. 16, pp. 264–270, 2002.

[13] G. Campbell, M. McLure, and E. Newell, "Compressive behavior after simulated service conditions of some foamed materials intended as orthotic shoe insoles," *J. Rehab. Res. Develop.*, vol. 21, pp. 57–65, 1984.

[14] E. Chantelau and P. Haage, "An audit of cushioned diabetic footwear: Relation to patient compliance," *Diabet. Med.*, vol. 11, pp. 114–116, 1994.

[15] *FSA Pressure Mapping System User's Manual*, vol. 8, Vista Medical Ltd., Winnipeg, MB, Canada, 2003, p. 58.

[16] S. Haykin, *Adaptive Filter Theory*. Upper Saddle River, NJ: Prentice-Hall, 2002, ch. 1, 8, and 9.

[17] *Neural Networks Toolbox (4.0) User's Guide*. Natick, MA: The MathWorks, 2000, ch. 2, 5, 6, and 11.

Aimee L. Betker (M'02) received both the B.Sc. (2002) and M.Sc. (2004) degrees from the University of Manitoba, Winnipeg, MB, Canada, in computer and electrical engineering, respectively. Currently, she is continuing her studies at the University of Manitoba, Department of Electrical and Computer Engineering, toward the Ph.D. degree in electrical engineering.

Her current research interests include the development of a simple tool and test protocol that will permit reliable evaluation of balance and movement interaction on different support surfaces, for a hierarchy of increasing dynamics and functional tasks. In addition, the investigation of how these different support surface mediums affect foot functions and balance control, for application to the development of corrective footwear.

Ms. Betker is a member of IEEE and Engineering in Medicine and Biology Society (EMBS). In 2004 she received a Manitoba Health Research Council (MHRC) Award for work on the Ph.D. thesis project.

Zahra M. K. Moussavi (M'98) received the B.Sc. degree from Sharif University of Technology, Tehran, Iran, in 1987, the M.Sc. degree from the University of Calgary, Calgary, AB, Canada, in 1993, and the Ph.D. degree from University of Manitoba, Winnipeg, MB, Canada in 1997, all in electrical engineering.

She then joined the respiratory research group of the Winnipeg Children's Hospital and worked as a Research Associate for one and a half years. In 1999, she joined the Biomedical Engineering Department of Johns Hopkins University, Baltimore, MD, and worked there as a Postdoctoral Fellow for one year. Following that, she joined the University of Manitoba, Department of Electrical and Computer Engineering as a faculty member, where she is currently an Assistant Professor. She is also an Adjunct Professor at the TR lab of Winnipeg. Her current research includes respiratory and swallowing sound analysis, postural control and balance, rehabilitation and human motor learning.

Dr. Moussavi is a member of IEEE, Engineering in Medicine and Biology (EMBS), CMBES, and International Lung Sound (ILSA) associations. She is also currently the EMBS Chapter Chair, Winnipeg Section.

Tony Szturm was born in Thunder Bay Ontario, Canada. He received the B.Sc. degree in biology and the B.Sc. degree in physical therapy from the University of Western Ontario, London, ON, Canada, 1980. He received the Ph.D. degree in neurophysiology from the University of Manitoba, Winnipeg, MB, Canada, in1988.

He worked as a Physiotherapist from 1980 to 1984, at Health Sciences Centre, Winnipeg, MB. Presently, he is an Associate Professor with the School of Medical Rehabilitation, University of Manitoba, and Adjunct Professor with the Department of Electrical and Computer Engineering and Department of Physiology. His research focus is in the field of human postural control in health and disease. The basis of this research is neuroscience, rehabilitation science, and dynamics of human movement; in particular, the integration of balance and mobility during standing tasks and walking. Another research aim is to better understand adaptive plasticity after neurological injury and the neural mechanisms responsible for behavioral recovery.

Dr. Szturm is a member of the College of Physiotherapy of Manitoba, Canadian Physiotherapy Association, and International Society of Posture and Gait.